An efficient approach for reliability-based optimization of linear dynamical structures subject to Gaussian excitation

Danko Jerez
Institute for Risk and Reliability, Leibniz Universität Hannover, 30167 Hannover, Germany, danko.jerez@irz.uni-hannover.de.

Hector Jensen
Department of Civil Engineering, Santa Maria University, 2390302 Valparaiso, Chile, hector.jensen@usm.cl.
International Joint Research Center for Engineering Reliability and Stochastic Mechanics, Tongji University, 200092 Shanghai, China.

Marcos Valdebenito
Faculty of Engineering and Sciences, Universidad Adolfo Ibáñez, 2562340 Viña del Mar, Chile, marcos.valdebenito@uai.cl

Mauricio Misraji
Department of Civil Engineering, Santa Maria University, 2390302 Valparaiso, Chile, mauricio.misraji@alumnos.usm.cl.

Michael Beer
Institute for Risk and Reliability, Leibniz Universität Hannover, 30167 Hannover, Germany, beer@irz.uni-hannover.de.
International Joint Research Center for Engineering Reliability and Stochastic Mechanics, Tongji University, 200092 Shanghai, China.
Institute for Risk and Uncertainty, School of Engineering, University of Liverpool, L69 7ZF Liverpool, United Kingdom.

Abstract. One pivotal task of structural engineering is to devise optimal structures according to a given criterion, while satisfying certain performance requirements that take into account all related uncertainties. This work proposes an efficient approach for reliability-based optimization of linear dynamical structures subject to stochastic Gaussian excitation, where the constraints are given in terms of first-excursion probabilities. Directional Importance Sampling (DIS) is considered for reliability assessment, which also estimates the reliability sensitivities as a by-product. The simulation technique is coupled with an efficient feasible-direction interior-point algorithm, in which every iteration provides a better design that is also feasible. The capabilities of the proposed approach are demonstrated by means of an illustrative example.

Keywords: reliability-based optimization, first-passage probabilities, gradient-based algorithms.

1. Introduction

Structural systems are usually devised to be optimum in terms of a certain criterion while satisfying given performance conditions (Haftka and Gürdal, 1992). In many applications, stochastic excitation models are considered and the corresponding requirements on the structural performance are expressed in terms of reliability measures (Suksuwan and Spence, 2018). In such cases, a reliability-based optimization (RBO) problem must be solved to obtain the optimum structural design (Jensen, 2005). These systems are associated with a high number of uncertain parameters (in the order of hundreds or thousands) and, therefore, simulation-based approaches (Schuëller and Pradlwarter, 2007) must be implemented to assess their reliability. As a result, these problems are highly involved from the numerical viewpoint.

Several approaches have been proposed in the literature to deal with the RBO of structural systems under stochastic excitation. Some of them include gradient-based schemes (Jensen et al., 2013), formulations in the so-called augmented reliability space (Ching and Hsieh, 2007) and stochastic optimization approaches (Taflanidis and Beck, 2008). Although the previous contributions have shown different levels of effectiveness, it is believed that there is still room for further developments in this area.

Attention is directed towards RBO problems involving deterministic linear structural systems under Gaussian excitation (Au and Beck, 2001). In this context, the present contribution proposes a framework that integrates a feasible-direction interior-point algorithm (Herskovits et al., 2011, Jensen et al., 2013) with Directional Importance Sampling (DIS) for reliability and reliability sensitivity evaluation (Misraji et al., 2020, Misraji et al., 2019). An illustrative example is considered to demonstrate the capabilities of the proposed approach.

The document is organized as follows. The class of problems of interest is formulated in Section 2. Section 3 discusses the optimization strategy. The main aspects of Directional Importance Sampling for reliability and reliability sensitivity estimation are discussed in Sections 4 and 5, respectively. An illustrative example is studied in Section 6. The paper closes with some final remarks.

2. Problem formulation

Consider the inequality-constrained nonlinear optimization problem

$$\begin{array}{ll} \min_{\mathbf{x}} & c(\mathbf{x}) \\ \text{s.t.} & g_j(\mathbf{x}) \leq 0,\ j=1,\ldots,n_g \\ & r_j(\mathbf{x}) \leq 0,\ j=1,\ldots,n_r \\ & x_i^l \leq x_i \leq x_i^u,\ i=1,\ldots,n_x \end{array} \tag{1}$$

where $\mathbf{x} = \langle x_1, \ldots, x_{n_x} \rangle^T$ is the vector of n_x design or control variables associated with the structural system, $c(\mathbf{x})$ is a general cost function, $g_j(\mathbf{x}) \leq 0, j = 1, \ldots, n_g$ represent the n_g standard constraints, $r_j(\mathbf{x}) \leq 0, j = 1, \ldots, n_r$ correspond to the n_r constraints on the system reliability, and $x_i^l \leq x_i \leq x_i^u, i = 1, \ldots, n_x$ are the side constraints on the design variables. It is assumed that all the functions involved in (1) vary smoothly in terms of the design variables and that the evaluation of the reliability constraints involves considerable numerical efforts.

2.1. Reliability constraints

The reliability constraint functions are expressed as $r_j(\mathbf{x}) = P^*_{F_j} - P_{F_j}(\mathbf{x}), j = 1, \dots, n_r$, where $P_{F_j}(\mathbf{x})$ is the failure probability function with maximum allowable value $P^*_{F_j}$. First-passage failure probabilities within a reference period T are considered. Thus, the failure events are given by

$$F_j(\mathbf{x}) = \{\boldsymbol{\theta} \in \Omega_\theta : d_j(\mathbf{x}, \boldsymbol{\theta}) \geq 1\}, \quad j = 1, \dots, n_r \tag{2}$$

where $\boldsymbol{\theta} \in \Omega_\theta \subset \mathbb{R}^{n_\theta}$ is the vector of random variables and the normalized demand function is

$$d_j(\mathbf{x}, \boldsymbol{\theta}) = \max_{\ell=1,\dots,n_j} \max_{t \in [0,T]} \frac{|h_{j,\ell}(t; \mathbf{x}, \boldsymbol{\theta})|}{h^*_{j,\ell}} \tag{3}$$

where $h_{j,\ell}(t; \mathbf{x}, \boldsymbol{\theta}), \ell = 1, \dots, n_j$ are the response functions with maximum allowable thresholds $h^*_{j,\ell} > 0$. Thus, the normalized demand function d_j quantifies the maximum demand-to-capacity ratio observed during the reference period T across all the responses of interest. The corresponding failure probability function is given by $P_{F_j}(\mathbf{x}) = \int_{d_j(\mathbf{x},\boldsymbol{\theta}) \geq 1} p(\boldsymbol{\theta}) d\boldsymbol{\theta}$, where $p(\boldsymbol{\theta})$ is the multivariate probability density function of the basic random variables. Since $\boldsymbol{\theta}$ is high-dimensional (in the order of hundreds or thousands), the previous integral is very challenging to evaluate. To this end, DIS is adopted here (Misraji et al., 2020), whose most salient features are given in Section 4.

3. Optimization strategy

A first-order feasible-direction interior-point algorithm is considered in the present implementation (Herskovits et al., 2011). Starting from a feasible design, each iteration identifies a feasible design with lower objective function value. The algorithm is based on the Karush-Kuhn-Tucker (KKT) first-order optimality conditions corresponding to the optimization, which can be stated as (Herskovits et al., 2011)

$$\begin{array}{l} \nabla c(\mathbf{x}) + \boldsymbol{\nabla}\mathbf{g}(\mathbf{x})\boldsymbol{\lambda}_g + \boldsymbol{\nabla}\mathbf{r}(\mathbf{x})\boldsymbol{\lambda}_r = \mathbf{0} \\ \mathbf{G}(\mathbf{x})\boldsymbol{\lambda}_g = \mathbf{0}, \qquad \mathbf{R}(\mathbf{x})\boldsymbol{\lambda}_r = \mathbf{0} \\ g_j(\mathbf{x}) \leq 0, \quad j = 1, \dots, n_g \\ r_j(\mathbf{x}) \leq 0, \quad j = 1, \dots, n_r \\ \boldsymbol{\lambda}_g \geq \mathbf{0}, \quad \boldsymbol{\lambda}_r \geq \mathbf{0} \end{array} \tag{4}$$

where $\boldsymbol{\lambda}_g \in \mathbb{R}^{n_g}$ and $\boldsymbol{\lambda}_r \in \mathbb{R}^{n_r}$ are the vectors of dual variables, $\boldsymbol{\nabla}\mathbf{g}(\mathbf{x}) \in \mathbb{R}^{n_x \times n_g}$ and $\boldsymbol{\nabla}\mathbf{r}(\mathbf{x}) \in \mathbb{R}^{n_x \times n_r}$ are the matrices of the derivatives of the standard and reliability constraint functions, respectively, given by $\boldsymbol{\nabla}\mathbf{g}(\mathbf{x}) = [\nabla g_1(\mathbf{x}), g_2(\mathbf{x}), \dots, g_{n_g}(\mathbf{x})]$ and $\boldsymbol{\nabla}\mathbf{r}(\mathbf{x}) = [\nabla r_1(\mathbf{x}), r_2(\mathbf{x}), \dots, r_{n_r}(\mathbf{x})]$, and $\mathbf{G}(\mathbf{x}) \in \mathbb{R}^{n_g \times n_g}$ and $\mathbf{R}(\mathbf{x}) \in \mathbb{R}^{n_r \times n_r}$ are diagonal matrices such that $G_{jj}(\mathbf{x}) = g_j(\mathbf{x}), j = 1, \dots, n_g$ and $R_{jj}(\mathbf{x}) = r_j(\mathbf{x}), j = 1, \dots, n_r$.

At each iteration, three main tasks are carried out. First, a feasible-descent direction is computed (Section 3.1). Then, the step length along the feasible-descent direction is determined based on an inexact line search procedure (Section 3.2). Finally, some auxiliary variables are updated (Section 3.3). Further implementation details can be found in (Herskovits et al., 2011, Jensen et al., 2013).

3.1. Feasible-descent direction

At the beginning of the k-th optimization cycle, $k = 0, 1, \ldots$, a feasible-descent direction is generated as $\mathbf{d}^k = \mathbf{d}_1^k + \rho^k \mathbf{d}_2^k$, where $\mathbf{d}_1^k$ is a descent direction of the objective function $c(\mathbf{x})$, $\mathbf{d}_2^k$ is a vector pointing towards the interior of the feasible domain and $\rho^k > 0$. The vectors $\mathbf{d}_1^k$ and $\mathbf{d}_2^k$ are obtained by solving

$$\begin{bmatrix} \mathbf{B}^k & \boldsymbol{\nabla}\mathbf{g}(\mathbf{x}^k) & \boldsymbol{\nabla}\mathbf{r}(\mathbf{x}^k) \\ \boldsymbol{\Lambda}_g^k \boldsymbol{\nabla}\mathbf{g}(\mathbf{x}^k)^T & \mathbf{G}(\mathbf{x}^k) & \mathbf{0} \\ \boldsymbol{\Lambda}_r^k \boldsymbol{\nabla}\mathbf{r}(\mathbf{x}^k)^T & \mathbf{0} & \mathbf{R}(\mathbf{x}^k) \end{bmatrix} \begin{Bmatrix} \mathbf{d}_1^k \\ \bar{\boldsymbol{\lambda}}_{g1}^{k+1} \\ \bar{\boldsymbol{\lambda}}_{r1}^{k+1} \end{Bmatrix} = - \begin{Bmatrix} \nabla c(\mathbf{x}^k) \\ \mathbf{0} \\ \mathbf{0} \end{Bmatrix} \tag{5}$$

$$\begin{bmatrix} \mathbf{B}^k & \boldsymbol{\nabla}\mathbf{g}(\mathbf{x}^k) & \boldsymbol{\nabla}\mathbf{r}(\mathbf{x}^k) \\ \boldsymbol{\Lambda}_g^k \boldsymbol{\nabla}\mathbf{g}(\mathbf{x}^k)^T & \mathbf{G}(\mathbf{x}^k) & \mathbf{0} \\ \boldsymbol{\Lambda}_r^k \boldsymbol{\nabla}\mathbf{r}(\mathbf{x}^k)^T & \mathbf{0} & \mathbf{R}(\mathbf{x}^k) \end{bmatrix} \begin{Bmatrix} \mathbf{d}_2^k \\ \bar{\boldsymbol{\lambda}}_{g2}^{k+1} \\ \bar{\boldsymbol{\lambda}}_{r2}^{k+1} \end{Bmatrix} = - \begin{Bmatrix} \mathbf{0} \\ \boldsymbol{\lambda}_g^k \\ \boldsymbol{\lambda}_r^k \end{Bmatrix} \tag{6}$$

where $\left(\mathbf{x}^k, \boldsymbol{\lambda}_g^k, \boldsymbol{\lambda}_r^k\right)$ is the starting point at the k-th iteration, $\boldsymbol{\Lambda}_g^k$ and $\boldsymbol{\Lambda}_r^k$ are diagonal matrices with coefficients $\Lambda_{gii}^k = \lambda_{gi}^k, i = 1, \ldots, n_g$ and $\Lambda_{rii}^k = \lambda_{ri}^k, i = 1, \ldots, n_r$, and $\mathbf{B}^k$ is a symmetric and positive definite matrix. An upper bound on ρ^k is established in order to ensure that $\mathbf{d}^k$ is a descent direction (Herskovits et al., 2011, Jensen et al., 2013), which is given by $\rho_{\text{limit}}^k = (\alpha - 1)\mathbf{d}_1^{k^T} \nabla c(\mathbf{x}^k) / (\mathbf{d}_2^{k^T} \nabla c(\mathbf{x}^k))$, with $\alpha \in (0, 1)$.

It is noted that the coefficient matrix of equations (5) and (6) involves the first-order derivatives of the reliability constraints. These quantities can be obtained as a by-product of DIS (Misraji et al., 2019). The main ideas of this approach are discussed in Section 5.

3.2. Line search

Once the search direction $\mathbf{d}^k$ is determined, the new candidate design is computed as $\mathbf{x}^{k+1} = \mathbf{x}^k + \tau_k \mathbf{d}^k$ where $\tau_k > 0$ is the step length along the feasible-descent direction. This quantity is obtained by means of a constrained line search procedure (Nocedal and Wright, 2006).

For each candidate step length τ_{cand}, the Armijo's criterion (Armijo, 1966) is first checked. This provides an upper bound for the step length. In addition, τ_{cand} must verify the Wolfe's criterion (Wolfe, 1969), which indicates a lower bound for the step length.

If Armijo's and Wolfe's criteria are simultaneously verified, then $\tau_k = \tau_{\text{cand}}$. Otherwise, a new candidate step length is obtained by solving the optimization problem

$$\begin{aligned} \max_{\tau} \quad & \tau \\ \text{s.t.} \quad & g_j(\mathbf{x}^k + \tau \mathbf{d}^k) \leq 0, \quad j = 1, \ldots, n_g \\ & \tilde{r}_j(\tau) \leq 0, \quad j = 1, \ldots, n_r \end{aligned} \tag{7}$$

where τ^L and τ^R are lower and upper limits for the step length, respectively, and $\tilde{r}_j(\tau)$ is an approximation of r_j along $\mathbf{d}^k$. The reader is referred to (Jensen et al., 2013) for further details.

3.3. Auxiliary variables updating

Once a new candidate design $\mathbf{x}^{k+1}$ has been determined, $\boldsymbol{\lambda}_g^{k+1}$ and $\boldsymbol{\lambda}_r^{k+1}$ are updated considering the scheme proposed in (Herskovits et al., 2011), while the positive definite matrix $\mathbf{B}^{k+1}$ is computed using a Broyden–Fletcher–Goldfarb–Shanno-type of formula (Nocedal and Wright, 2006).

4. Reliability estimation

The type of stochastic loading considered in this contribution corresponds to a Gaussian process. Thus, this loading is actually a linear function with respect to $\boldsymbol{\theta}$, which follows a standard normal distribution in n_θ dimensions. Furthermore, the type of structural systems considered in this contribution exhibits a linear behavior. Under these assumptions, it is straightforward to show that the response $h_{j,\ell}(t;\mathbf{x},\boldsymbol{\theta})$ is linear with respect to $\boldsymbol{\theta}$ at each time instant of analysis and for a given value of the design variables $\mathbf{x}$ (Au and Beck, 2001). Hence, the failure domain is bounded by a series of hyperplanes, as represented schematically in Figure 1.

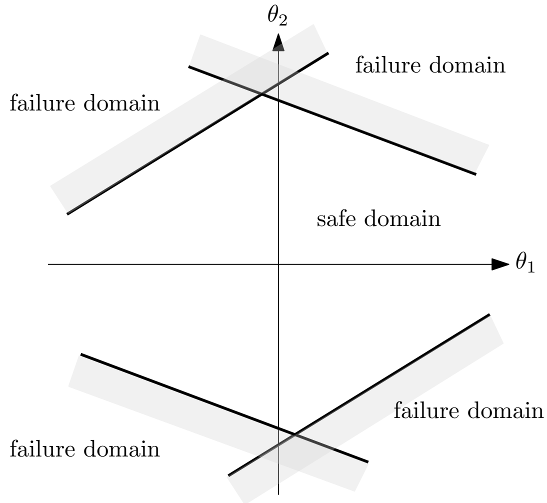

Figure 1. Schematic representation of failure domain

Taking into account the geometry of the failure domain, the probability integral can be formulated within the framework of Directional Importance Sampling, that is:

$$P_{F_j}(\mathbf{x}) = \int_{\boldsymbol{\zeta}\in\Omega_{\mathbf{Z}}} \int_{\psi_j^*(\mathbf{x},\boldsymbol{\zeta})}^{\infty} p_\Psi(\psi) \frac{p_{\mathbf{Z}}(\boldsymbol{\zeta})}{p_{\mathbf{Z}}^{\mathrm{IS}}(\boldsymbol{\zeta})} p_{\mathbf{Z}}^{\mathrm{IS}}(\boldsymbol{\zeta}) d\psi d\boldsymbol{\zeta} \tag{8}$$

where $\boldsymbol{\zeta}$ is a unit vector that points in the direction of $\boldsymbol{\theta}$, with associated probability distribution $p_{\mathbf{Z}}(u)$; $\Omega_{\mathbf{Z}}$ is the set of all points belonging to the unit hypersphere; ψ is the Euclidean norm of $\boldsymbol{\theta}$, with associated probability distribution $p_\Psi(\psi)$; $\psi_j^*(\mathbf{x},\boldsymbol{\zeta})$ is the value of ψ that fulfills the equation $d_j(\mathbf{x},\psi\boldsymbol{\zeta}) = 1$; and where $p_{\mathbf{Z}}^{\mathrm{IS}}(\boldsymbol{\zeta})$ is the importance sampling density function associated with the direction vector. The importance sampling density function is equal to a weighted summation of the probability density function associated with $\boldsymbol{\zeta}$ conditioned on the occurrence of the failure event at each discrete time instant. It can be shown that explicit expressions associated with $p_{\mathbf{Z}}^{\mathrm{IS}}(\boldsymbol{\zeta})$ can be deduced by means of Bayes' theorem, as discussed in (Misraji et al., 2020). Thus, it is possible to evaluate the probability in equation (8) by means of simulation. Numerical experience indicates that a few hundreds of samples allow producing highly accurate estimates of the sought probability.

5. Reliability sensitivity estimation

The structure of equation (8) reveals that the failure probability P_{F_j} depends on the value of the design variable vector $\mathbf{x}$. This is clear from a physical viewpoint, as changes to this vector affect the response of the structure, which in turn affect the probability. Undoubtedly, assessing the rate of change of this probability with respect to changes in this design vector provides valuable information for decision making. Formally, such rate of change can be expressed in terms of the gradient, that is:

$$\frac{\partial P_{F_j}(\mathbf{x})}{\partial x_i} = \frac{\partial}{\partial x_i}\left(\int_{\boldsymbol{\zeta}\in\Omega_{\mathbf{Z}}}\int_{\psi_j^*(\mathbf{x},\boldsymbol{\zeta})}^{\infty} p_{\Psi}(\psi)\frac{p_{\mathbf{Z}}(\boldsymbol{\zeta})}{p_{\mathbf{Z}}^{\mathrm{IS}}(\boldsymbol{\zeta})}p_{\mathbf{Z}}^{\mathrm{IS}}(\boldsymbol{\zeta})d\psi d\boldsymbol{\zeta}\right),\ i=1,\ldots,n_x \tag{9}$$

The above integral can be simplified resorting to the Leibniz rule for differentiation, leading to an integral over the hypersurface that separates the safe and failure domains and that comprises the derivative of the normalized demand function $d_j(\mathbf{x}, \psi\boldsymbol{\zeta})$ with respect to x_i. The integral over the hypersurface is solved straightforwardly within the framework of Directional Importance Sampling, as this simulation technique tracks (by definition) the aforementioned hypersurface. Moreover, the derivative of the normalized demand function can be easily calculated by considering the sensitivity of the spectral properties (natural frequencies and mode shapes of the structure), as discussed in (Lee and Jung, 1997).

In summary, the sensitivity of the failure probability as cast in equation (9) is calculated with all the information produced when calculating the failure probability itself plus the sensitivity of the response with respect to the design variables. In other words, the sensitivity of the probability becomes a by-product of the reliability analysis.

6. Illustrative example

6.1. Problem description

The illustrative example considered in this work addresses the optimum design of a two-degree-of-freedom linear system subject to Gaussian excitation. The system is shown in Figure 2. The mass of each floor is $m = 30 \times 10^3$ kg, k_1 and k_2 represent the stiffnesses of the first and second story, respectively, and $u_i, i = 1, 2$ are the ground-relative displacements at the different floors. In addition, a 4% of the critical damping is considered at the modal level.

The structural system is subject to stochastic ground acceleration modeled as a modulated white noise process that passes through a Clough-Penzien type of filter. Specifically, $\ddot{u}_g(t) = \Omega_1^2 w_1(t) +$

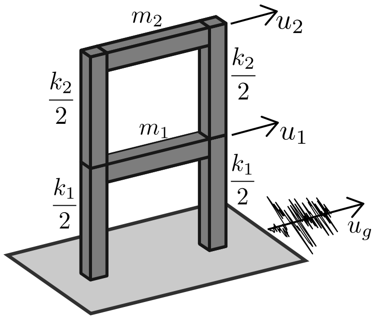

Figure 2. Two-degree-of-freedom system

$2\xi_1\Omega_1\dot{w}_1(t) - \Omega_2^2 w_2(t) - 2\xi_2\Omega_2\dot{w}_2(t)$, where $\Omega_1 = 15.6$ rad/s, $\xi_1 = 0.6$ are the parameters of the first filter, and $\Omega_2 = 1.0$ rad/s, $\xi_2 = 0.9$ are the parameters of the second filter. The white noise process has an intensity $S = 10^{-4}$ m^2/s^3, a duration $T = 15$ s and a time step $\Delta t = 0.01$ s. The time envelope function $h(t)$ is given by

$$h(t) = \begin{cases} (t/5)^2 & 0 \leq t \leq 5\text{s} \\ 1 & 5 < t \leq 10\text{s} \\ e^{-(t-10)^2} & t > 10\text{s} \end{cases} \tag{10}$$

The objective of this example is to minimize the structural cost with respect to the interstory stiffnesses under a reliability constraint associated with the top displacement, that is,

$$\begin{array}{cl} \max\limits_{\mathbf{x}=\langle x_1,x_2\rangle^T} & c(\mathbf{x}) \\ \text{s.t.} & P_F(\mathbf{x}) \leq P_F^* \\ & 0.5 \leq x_i \leq 1.5, \quad i = 1,2 \end{array} \tag{11}$$

where $c(\mathbf{x})$ is the cost function and $P_F(\mathbf{x})$ is the failure probability function with maximum allowable value $P_F^* = 10^{-3}$. The design variables are defined as the interstory stiffnesses normalized with respect to a reference value. Specifically, $x_i = k_i/\bar{k}, i = 1,2$, with $\bar{k} = 18 \times 10^6$ N/m. For illustration purposes, the cost function is assumed to be proportional to the normalized interstory stiffnesses. In particular, $c(\mathbf{x}) = x_1 + x_2$. Finally, the failure event is defined as $F = \{\boldsymbol{\theta} \in \Omega_\theta : d(\mathbf{x}, \boldsymbol{\theta}) > 1\}$, where $d(\mathbf{x}, \boldsymbol{\theta}) = \max_{t\in[0,T]} |u_2(t; \mathbf{x}, \boldsymbol{\theta})| / u_2^*$ and $u_2^* = 0.006$ m.

6.2. Results and discussion

In order to gain insight into the system under analysis, Figure 3 (left) shows the contours of the failure probability function in the design space. These curves have been smoothed for presentation purposes. The structure becomes more reliable for higher stiffness values and some interaction between the design variables is observed. This behavior is reasonable from a physical viewpoint, since the response of interest corresponds to the top displacement. In addition, a sketch of the feasible design space and some contours of the objective function are depicted in Figure 3 (right).

The optimization process is carried out considering the initial solution $\mathbf{x}^0 = \langle 1.4, 1.4\rangle^T$ and a total of 1000 samples for the implementation of DIS. The trajectory of the candidate solutions in the

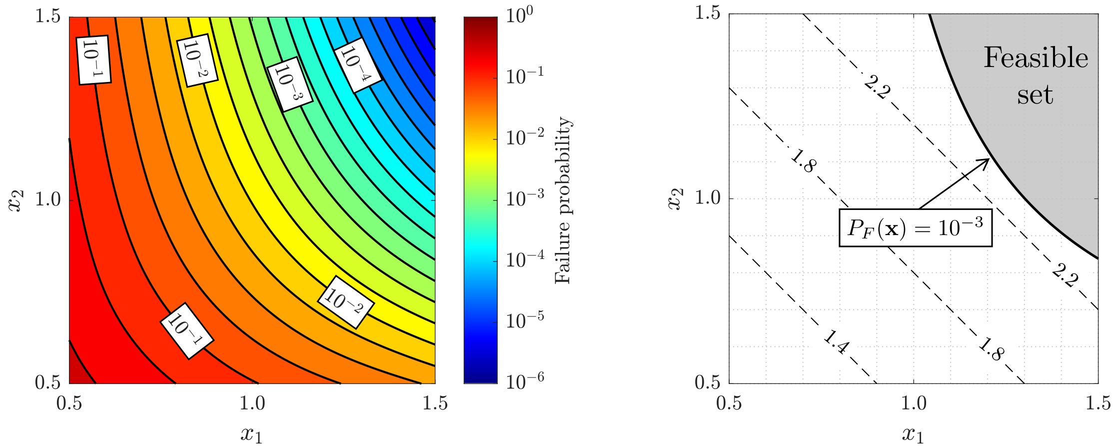

Figure 3. Left: Iso-probability curves. Right: Sketch of the feasible design space

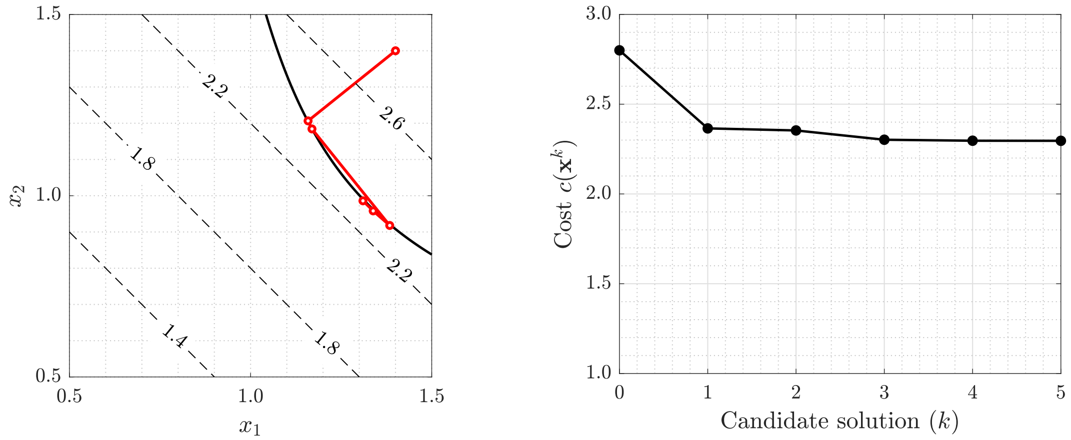

Figure 4. Candidate designs (left) and optimum costs (right) obtained during the optimization process

design space is shown in Figure 4 (left), where some contours of the cost function have been included with dashed lines. The initial search direction is orthogonal to the cost contours. Afterwards, the designs move nearly parallel to the reliability constraint. The corresponding objective function values are shown in Figure 4 (right). Most of the improvements of the objective function take place during the first steps of the optimization scheme. The final design is obtained after five iterations and is given by $\mathbf{x}^* = \langle 1.31, 0.98 \rangle^T$, with $P_F(\mathbf{x}^*) = 10^{-3}$ and $c(\mathbf{x}^*) = 2.29$.

7. Conclusions

This contribution has proposed an approach for reliability based design optimization of linear structures subject to dynamic Gaussian load. The proposed framework employs a first order optimization scheme which ensures that each candidate solution is feasible and better than the previous ones.

This scheme is integrated with Directional Importance Sampling, which is a simulation method which allows estimating first excursion probabilities and their gradients most efficiently.

The results presented in this contribution are encouraging, as it is possible to determine an optimal design solution with reduced numerical efforts. Nonetheless, the scope of application of the proposed approach remains to be verified in problems involving large scale structures. This issue is currently under investigation by the authors.

Acknowledgements

This research was supported in part by ANID (National Agency for Research and Development, Chile) under its program FONDECYT, grant numbers 1200087 and 1180271. Also, this research has been partially supported by ANID and DAAD (German Academic Exchange Service, Germany) under CONICYT-PFCHA/Doctorado Acuerdo Bilateral DAAD Becas Chile/2018-62180007.

References

Armijo, L.: 1966, ‘Minimization of Functions having Lipschitz Continuous First Partial Derivatives’. *Pacific Journal of Mathematics* **16**(1), 1–3.

Au, S. and J. Beck: 2001, ‘First excursion probabilities for linear systems by very efficient importance sampling’. *Probabilistic Engineering Mechanics* **16**(3), 193–207.

Ching, J. and Y. Hsieh: 2007, ‘Approximate Reliability-Based Optimization Using a Three-Step Approach Based on Subset Simulation’. *Journal of Engineering Mechanics* **133**(4), 481–493.

Haftka, R. and Z. Gürdal: 1992, *Elements of Structural Optimization.* Dordrecht, The Netherlands: Kluwer, 3^{rd} edition.

Herskovits, J., W. Freire, M. Fo, and A. Canelas: 2011, ‘A feasible directions method for nonsmooth convex optimization’. *Structural and Multidisciplinary Optimization* **44**(3), 363–377.

Jensen, H.: 2005, ‘Structural optimization of linear dynamical systems under stochastic excitation: a moving reliability database approach’. *Computers Methods in Applied Mechanics and Engineering* **194**(12-16), 1757–1778.

Jensen, H., L. Becerra, and M. Valdebenito: 2013, ‘On the Implementation of an Advanced Interior Point Algorithm for Stochastic Structural Optimization’. *Computers & Structures* **126**, 69–85.

Lee, I.-W. and G.-H. Jung: 1997, ‘An efficient algebraic method for the computation of natural frequency and mode shape sensitivities - Part I. Distinct natural frequencies’. *Computers & Structures* **62**(3), 429–435.

Misraji, M., M. Valdebenito, H. Jensen, and C. Mayorga: 2020, ‘Application of directional importance sampling for estimation of first excursion probabilities of linear structural systems subject to stochastic Gaussian loading’. *Mechanical Systems and Signal Processing* **139**, 106621.

Misraji, M., M. Valdebenito, C. Mayorga, and H. Jensen: 2019, ‘Reliability Sensitivity Analysis for Linear Structures Subject to Dynamic Gaussian Excitation’. In: *29th European Safety and Reliability Conference (Esrel 2019).* Hannover, Germany.

Nocedal, J. and S. Wright: 2006, *Numerical Optimization.* New York: Springer New York, 2nd edition.

Schuëller, G. and H. Pradlwarter: 2007, ‘Benchmark Study on Reliability Estimation in Higher Dimensions of Structural Systems – An Overview’. *Structural Safety* **29**, 167–182.

Suksuwan, A. and S. Spence: 2018, ‘Optimization of uncertain structures subject to stochastic wind loads under system-level first excursion constraints: A data-driven approach’. *Computers & Structures* **210**, 58 – 68.

Taflanidis, A. and J. Beck: 2008, ‘An efficient framework for optimal robust stochastic system design using stochastic simulation’. *Computer Methods in Applied Mechanics and Engineering* **198**(1), 88–101.

Wolfe, P.: 1969, ‘Convergence Conditions for Ascent Methods’. *SIAM Review* **11**(2), 226–235.